DOI: 10.1021/ic101027d

Inorganic Chemistry
Article

# $\{Mo_{96}La_8\}$ Eggshell Ring and Self-Assembly to $\{Mo_{132}\}$ Keplerate through Mo-blue Intermediate, Involved in UV-Photolysis of $[Mo_7O_{24}]^{6-}$/Carboxylic Acid System at pH 4

**Toshihiro Yamase,*,†,‡ Shun Kumagai,† Petra V. Prokop,† Eri Ishikawa,†,§ and Adrian-Raul Tomsa†**

†*Tokyo Institute of Technology, Chemical Resources Laboratory, R1-21, 4259 Nagatsuta, Midori-ku, Yokohama 226-8503 Japan,* ‡*MO Device (Inc.), 2-14-10 Kanaiwa-higashi Kanazawa, 920-0335 Japan, and* §*Chubu University, Department of Applied Chemistry, 1200 Matsumoto-cho, Kasugai, 487-8501 Japan*

Received May 20, 2010

The prolonged UV-photolysis of aqueous solutions containing $[Mo_7O_{24}]^{6-}$ and $C_2H_5CO_2H$ (as electron donor) at pH 3.9−4.1 generates the carboxylate-coordinated $\{Mo_{132}\}$ Keplerate (**1a**) isolated as a formamidinium/ammonium-mixed salt, $[HC(NH_2)_2]_{26}(NH_4)_{28}[Mo^{V}_{60}Mo^{VI}_{72}O_{372}(H_2O)_{48}(C_2H_5CO_2)_{36}(^{i}C_3H_7CO_2)_6]\cdot 16H_2O$ (**1**), through the Mo-blue intermediate (**2**). The coordination of **2** to $La^{3+}$ gives rise to the formation of the chain structure of the $C_2$-symmetric $\{Mo_{96}La_8\}$ eggshell rings, formulated by $H_{22}[Mo^{V}_{20}Mo^{VI}_{76}O_{301}(H_2O)_{29}\{La(H_2O)_6\}_2]\{La(H_2O)_5\}_6]\cdot 54.5H_2O$ (**3**). The eggshell-ring geometry results from the insertion of $[Mo^{VI}_2O_7(H_2O)]^{2-}$ (spacer) into the equator outer ring of the wheel-shaped Mo-blue, and 10 $\{(Mo^{VI})(Mo^{VI}_5)\}$ pentagonal subunits alternately above and below the equator outer ring are connected by eight $La^{3+}$ and two $\{Mo^{VI}_2\}$ linkers within two inner rings. The neighboring eggshell rings are linked through two Mo−O−Mo bonds formed by dehydrative condensation between the $\{Mo^{VI}_2\}$ linkers to result in the chain structure. Together with the results of the elemental analysis and IR, electronic absorption, $^{13}C$ NMR, and ESI-MS spectra for **2**, the ring profile analysis of **3** let us identify **2** with a carbolylate-coordinated Mo-blue ring of high nuclearity. The $Mo^{VI}\rightarrow Mo^{V}$ photoreductive change of **2** to the 60-electron reduced Keplerate in the presence of $C_2H_5CO_2H$ involves both degradation of the outer ring and splitting of the binuclear linkers, which leads to the formation of $[(Mo^{VI})Mo^{VI}_5O_{21}(H_2O)_4(\text{carboxylate})]^{7-}$ pentagonal subunits and $[Mo^{V}_2O_4(\text{carboxylate})]^{+}/[Mo^{V}O_2(\text{carboxylate})_{1/2}]^{0.5+}$-mixed linkers for **1**.

## Introduction

Prolonged UV-photolysis of aqueous solutions containing isopolyoxomolybdates and electron donors leads to the formation of Mo-blues and -browns, which one depends on pH levels, starting molybdates, and electron donors. The photolyses of $[Mo_{36}O_{112}(H_2O)_{16}]^{8-}$ (= $\{Mo^{VI}_{36}\}$), $\beta$-$[Mo_8O_{26}]^{4-}$ (= $\{Mo^{VI}_8\}$), and $[Mo_7O_{24}]^{6-}$ (= $\{Mo^{VI}_7\}$) generate 32- and 28-electron ($e^-$) reduced wheel-shaped Mo-blue rings such as $\{Mo_{176}\}$, $\{Mo_{154}\}$, and $\{Mo_{142}\}$;[1a] 24-$e^-$ reduced Mo-brown of $\{Mo_{37}\}$;[1b] and 12-$e^-$ reduced Mo-brown of $\{Mo_{16}\}$,[1c] at pH ranges of 0.5−2, 3−4, and 5−6, respectively. Each photolysis for the starting molybdates dominant at the corresponding pH range in the presence of electron donors such as alkylammonium cations, alcohols, and carboxylic acids has been investigated from a stand point of clarification of the self-assembly mechanism in addition to the photochemical design for the polyoxometalates-based nanorings, which were at first developed by Müller et al.[2−5] The plausible reaction pathways to Mo-blues and -browns involved in UV-induced self-assembly have been discussed with a help of X-ray crystallography, single-crystal and time-resolved ESR spectroscopies, electrospray/cryospray ionization mass (ESI-MS and CSI-MS) spectrometry, and Mo K-edge XAFS spectrometry.[1,6−9] For example, the formation of $\{Mo_{176}\}$

*To whom correspondence should be addressed. Fax: +81-76-267-0468 and +45-921-4805. E-mail: yamase.modevice@nifty.com.

(1) (a) Yamase, T.; Prokop, P. *Angew. Chem., Int. Ed.* **2002**, *37*, 466. (b) Yamase, T.; Ishikawa, E. *Langmuir* **2000**, *16*, 9023. (c) Yamase, T.; Ishikawa, E. *Bull. Chem. Soc. Jpn.* **2008**, *81*, 983.

(2) (a) Müller, A.; Beugholt, C.; Koop, M.; Das, S. K.; Schmidtmann, M.; Bögge, H. *Z. Anorg. Allg. Chem.* **1999**, *625*, 1960. (b) Müller, A.; Krickemeyer, E.; Bögge, H.; Schmidtmann, M.; Beugholt, C.; Das, S. K.; Peters, F. *Chem.—Eur. J.* **1999**, *5*, 1496.

(3) Müller, A.; Das, S. K.; Krickemeyer, E.; Kuhlmann, C. In *Inorganic Syntheses*; Shapley, J., Ed.; John Wiley & Sons: New York, 2004; pp 191−220.

(4) Müller, A.; Kögerler, P.; Dress, A. W. M. *Coord. Chem. Rev.* **2001**, *222*, 193.

(5) Kögerler, P.; Müller, A. In *Polyoxometalate chemistry for nano-composite design*; Yamase, T., Pope, M. T., Eds.; KluwerAcademic/Plenum Pubs.: New York, 2002; pp 1−15.

(6) (a) Yamase, T.; Prokop, P.; Arai, Y. *J. Mol. Struct.* **2003**, *656*, 107. (b) Yamase, T. In *Polyoxometalate Molecular Science, NATO Science series*; Borrás-Alamenar, J. J., Coronado, E.; Müller, A., Pope, M. T., Eds.; Kluwer Academic Publishers: Dordrecht, The Netherlands, 2003; pp 201−222.

(7) Yamase, T.; Yano, Y.; Ishikawa, E. *Langmuir* **2005**, *21*, 7823.

(8) Ito, T.; Yamase, T. *Eur. J. Inorg. Chem.* **2009**, 5205.

(9) Mitani, Y.; Oka, K.; Shibata, Y.; Konishi, K.; Obaid, D. M.; Ishikawa, E.; Izumi, Y.; Yamase, T. *Chem. Lett.* **2010**, *39*, 132.


Published on Web 09/20/2010

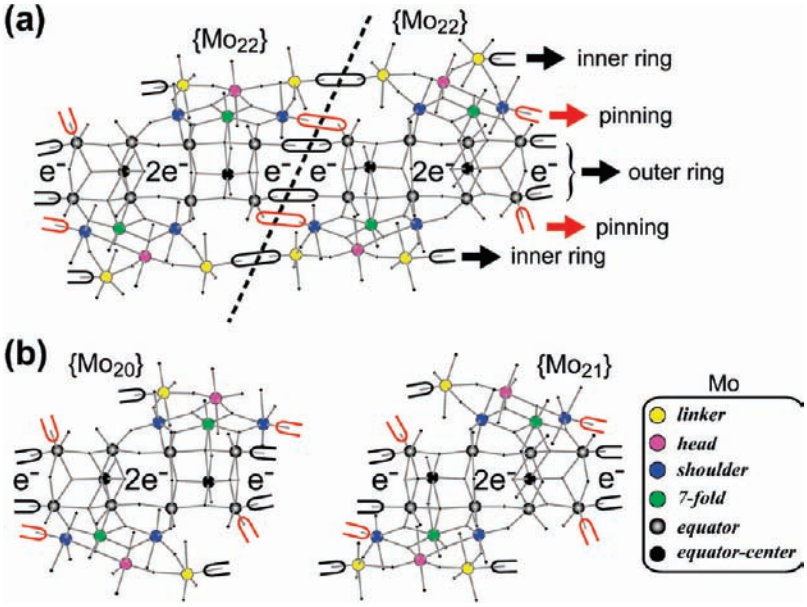


**Figure 1.** Dehydrative condensations among formally four-e$^-$ reduced $\{Mo_{22}\}$ building units to the wheel-shaped ring through the formation of three types of Mo−O−Mo bonds for the inner ring, outer ring, and pinning (a) and a schematic description of formally four-e$^-$ reduced $\{Mo_{20}\}$ and $\{Mo_{21}\}$ building blocks (b). Six types (*linker*, *head*, *shoulder*, *7-fold*, *equator*, and *equator-center*) of Mo atoms are indicated by different colored balls for clarification. O atoms surrounded by the half circle indicate OH groups for dehydrative condensation (with three types of black- and red-colored circles for the formation of outer and inner rings and pinning, respectively) between the two Mo−OH groups through the formation of a Mo−O−Mo bond.

(or $\{Mo_{154}\}$) as an intact ring circle at pH ≤ 1 has been elucidated by stepwise octameric (or heptameric) cyclic condensations among the formally four-e$^-$ reduced building blocks resulting from the two-e$^-$ photoreduction of $\{Mo_{22}\}$ (= $[Mo^{V}_{2}Mo^{VI}_{20}O_{60}(OH)_{12}(H_2O)_{10}]^{2-}$) through the construction of outer and inner rings, according to a mode similar to the two-e$^-$-reductive dimeric condensation of $\{Mo^{VI}_{7}\}$ to $[(Mo^{V}Mo^{VI}_{6}O_{23})_2]^{10-}$ (= $\{Mo_{14}\}$).[1a,10] Figure 1a shows a scheme of the dehydrative condensations among the formally four-e$^-$ reduced $\{Mo_{22}\}$ building blocks (= $[Mo^{V}_{4}Mo^{VI}_{18}O_{60}(OH)_{12}(H_2O)_{10}]^{4-}$) to the wheel-shaped ring together with the description of six types of Mo atoms (*linker*, *head*, *shoulder*, *7-fold*, *equator*, and *equator-center*).[11] In $\{Mo_{22}\}$, the aqua ligand is coordinated to each of the *linker*, *head*, and *shoulder* Mo atoms.[1a] The additional two-e$^-$ photoreduction of $\{Mo_{22}\}$, which formally consists of two $[(Mo^{VI})Mo^{VI}_{5}O_{22}(OH)_2(H_2O)_3]^{10-}$ (= $\{(Mo^{VI})(Mo^{VI}_{5})\}$) pentagonal sub-blocks above and below the equator comprising two $[Mo^{V}Mo^{VI}_{2}O_4(OH)_2]^{7+}$ fragments (of *equator* and *equator-center* Mo atoms) with the attachment of four $[Mo^{VI}O_2(OH)(H_2O)]^{+}$ linkers, occurs at two ends of the *equator* Mo atoms with a resultant formation of two $[Mo^{V}_{2}Mo^{VI}O_4(OH)_2]^{6+}$ fragments in the equator. The equator outer ring of the wheel-shaped ring is structurally assisted by the formation of two types of Mo−O−Mo bonds (i) between two *linker* Mo atoms (for the formation of the inner ring) and (ii) between *shoulder* and *equator* Mo atoms (for pinning). The formation of $\{Mo_{142}\}$ as a defect ring (comprising six defect pockets and eight binuclear $[Mo^{VI}_{2}O_5(H_2O)_2]^{2+}$ fragments (= $\{Mo^{VI}_{2}\}$) linkers within the inner ring) at pH 2 has been similarly demonstrated by cyclic condensation among the formally four-e$^-$ reduced building blocks of five $\{Mo_{20}\}$'s (= $[Mo^{V}_{4}Mo^{VI}_{16}O_{56}(OH)_{10}(H_2O)_8]^{6-}$) and two $\{Mo_{21}\}$'s (= $[Mo^{V}_{4}Mo^{VI}_{17}O_{58}(OH)_{11}(H_2O)_9]^{5-}$), as shown in Figure 1b, where the two-$\{(Mo^{VI})(Mo^{VI}_{5})\}$ pentagonal sub-blocks in $\{Mo_{20}\}$ and $\{Mo_{21}\}$ are attached by two and three $[Mo^{VI}O_2(OH)(H_2O)]^{+}$ linkers, respectively. Interestingly, the UV-photolysis of the $\{Mo^{VI}_{7}\}$/carboxylic acid system at pH 3.4 (where $\{Mo^{VI}_{8}\}$ is dominant) generates the caboxylate-coordinated $\{Mo_{142}\}$ ring, $[Mo^{V}_{28}Mo^{VI}_{114}O_{429}H_{10}(H_2O)_{49}(CH_3CO_2)_5(C_2H_5CO_2)]^{30-}$, implying that monomolybdates in equilibrium with $\{Mo^{VI}_{8}\}$ react with $\{Mo_{14}\}$ through the attachment of $MoO_4$ tetrahedra to form $\{Mo_{20}\}$ and $\{Mo_{21}\}$ building blocks.[7,9] Recently, we found the prolonged UV-photolysis of the $\{Mo^{VI}_{7}\}$/carboxylic acid system at pH 3.9−4.1 generates the 60-e$^-$ reduced $\{Mo_{132}\}$ Keplerate through the Mo-blue intermediate.

(10) Yamase, T. *J. Chem. Soc., Dalton Trans.* **1991**, 3055.

(11) The cyclic dehydrative condensations among the four-e$^-$ reduced $\{Mo_{22}\}$ building blocks to wheel-shaped Mo-blues rings undergo the formation of three types of Mo−O−Mo bonds for inner ring (by dehydrative condensation between two *linker* Mo atoms), outer ring (by dehydrative condensation between two *equator* Mo atoms), and "pinning" between *shoulder* and *equator* Mo atoms. The four-e$^-$ reduced $\{Mo_{22}\}$ building block has been formulated to be $[Mo^{V}_{4}Mo^{VI}_{18}O_{70}(H_2O)_{10}]^{12-}$,[7] in which the "pinning" type of the Mo−O−Mo bonds has been taken into consideration in advance for simplification. As suggested in the present work (on the Mo-blue intermediate), however, the Mo-blue ring is not always the closed ring. As exemplified by $[Mo^{V}_{4}Mo^{VI}_{18}O_{60}(OH)_{12}(H_2O)_{10}]^{4-}$ for $\{Mo_{22}\}$, Mo−OH groups are given in the formulas of four-e$^-$ reduced building blocks in this work, which account for the dehydrative condensation between Mo−OH groups through the formation of the three types of Mo−O−Mo bonds.

(12) (a) Müller, A.; Polarz, S.; Das, S. K.; Krickemeyer, E.; Bögge, H.; Schmidtmann, M.; Hauptfleisch, B. *Angew. Chem., Int. Ed.* **1999**, *38*, 3241. (b) Müller, A.; Sarkar, S.; Shah, S. Q. N.; Bögge, H.; Schmidtmann, M.; Sarkar, Sh.; Kögerler, P.; Hauptfleisch, B.; Trautwein, A. X.; Schünemann, V. *Angew. Chem., Int. Ed.* **1999**, *38*, 3238. (c) Müller, A.; Krickemeyer, E.; Bögge, H.; Schmidtmann, M.; Peters, F. *Angew. Chem., Int. Ed.* **1998**, *37*, 3360.

(13) (a) Müller, A. *Science* **2003**, *300*, 749. (b) Müller, A.; Krickemeyer, E.; Bögge, H.; Schmidtmann, M.; Botar, B.; Talismanova, M. O. *Angew. Chem., Int. Ed.* **2003**, *42*, 2085. (c) Müller, A.; Beckmann, E.; Bögge, H.; Schmidtmann, M.; Dress, A. *Angew. Chem., Int. Ed.* **2002**, *41*, 1162. (d) Müller, A.; Kögerler, P.; Kuhlmann, C. *Chem. Commun.* **1999**, 1347.

(14) In works on $\{Mo_{132}\}$, $\{(Mo^{VI})(Mo^{VI}_{5})\}$ and $\{Mo^{V}_{2}\}$ have been often called a pentagonal unit and spacer, respectively.[12,13,15] In this work, however, the " spacer" is defined for $\{Mo_{96}La_6\}$, and $\{(Mo^{VI})(Mo^{VI}_{5})\}$ and $\{Mo^{V}_{2}\}$ components are called a pentagonal subunit and linker, respectively, to avoid confusion.

The obtained $\{Mo_{132}\}$ Keplerate is the $I_h$-symmetric icosidodecahedral $\{(Mo^{VI})(Mo^{VI}_5)\}_{12}(linker)_{30}$, consisting of 12 $[(Mo^{VI})Mo^{VI}_5O_{21}(H_2O)_6]^{6-}$ (= $\{(Mo^{VI})(Mo^{VI}_5)\}$) pentagonal subunits and 30 binuclear $[Mo^{V}_2O_4(H_2O)_2]^{2+}$ (=$\{Mo^{V}_2\}$) linkers.[12−15] So far, the formation of the Keplerate has been understood formally to arise from the dehydrative condensations (to yield the $Mo^{V}(\mu_2\text{-}O)_2Mo^{V}$ bond accompanied by the $Mo^{V}-Mo^{V}$ bond between two mononuclear linkers) among 12 $\{[(Mo^{VI})Mo^{VI}_5O_{21}(H_2O)_6][Mo^{V}O(OH)_2(H_2O)]_5\}^{-}$ pentagon building blocks, each of which consists of a $\{(Mo^{VI})(Mo^{VI}_5)\}$ pentagonal subunit and five mononuclear $[Mo^{V}O(OH)_2(H_2O)]^{+}$ (= $\{Mo^{V}_1\}$) linkers.[12,13] To our knowledge, there has been no investigation of the origin of the above pentagon building block (or subunits) in the self-assembly of the Keplerate. We describe herein that the high nuclearity Mo-blue intermediate for $\{Mo_{132}\}$ is coordinated to $La^{3+}$ to yield a novel 20-e$^-$ reduced $\{Mo_{96}La_8\}$ eggshell-ring chain, which comprises 10 $\{(Mo^{VI})(Mo^{VI}_5)\}$ pentagonal subunits and two binuclear $\{Mo^{VI}_2\}$ linkers in each eggshell ring and gives a clue to the conformation change of the Mo-blue intermediate to the 60-e$^-$ reduced $\{Mo_{132}\}$ Keplerate through the $Mo^{VI}\rightarrow Mo^{V}$ photoreduction.

## Experimental Section

**Materials.** $[Me_3NH]_6[H_2Mo^{V}_{12}O_{28}(OH)_{12}(Mo^{VI}O_3)_4]\cdot 2H_2O$ (= $\{Mo_{16}\}$),[1c] $[^{i}PrNH_3]_{10}H_2[Mo^{V}_{28}Mo^{VI}_{114}O_{432}H_{28}(H_2O)_{58}]\cdot 90H_2O$ (= $\{Mo_{142}\}$),[1a] and $[NH_4]_{27}[Me_3NH]_3[Mo^{V}_{28}Mo^{VI}_{114}O_{429}H_{10}(H_2O)_{49}(CH_3CO_2)_5(C_2H_5CO_2)]\cdot(150\pm 10)H_2O$ (= $\{Mo_{142}(CH_3CO_2)_5(C_2H_5CO_2)\}$)[7] were photochemically prepared according to literature methods. All other chemicals were used as received unless otherwise stated.

**Preparation of $[HC(NH_2)_2]_{26}(NH_4)_{28}[Mo^{V}_{60}Mo^{VI}_{72}O_{372}(H_2O)_{48}(C_2H_5CO_2)_{36}(^{i}C_3H_7CO_2)_6]\cdot 16H_2O$ (1) and $H_{22}[Mo^{V}_{20}Mo^{VI}_{76}O_{301}(H_2O)_{29}\{La(H_2O)_6\}_2\{La(H_2O)_5\}_6]\cdot 54.5H_2O$ (= $\{Mo_{96}La_8\}$) (3).** Solid $[NH_4]_6[Mo_7O_{24}]\cdot 4H_2O$ (1.73 g, 1.4 mmol) was dissolved in water (35 mL), and propionic acid, $C_2H_5CO_2H$ (35 mL, 472 mmol), was added. The colorless solution adjusted to pH 3.9−4.1 with $NH_4OH$ was exposed at 10−15 °C under a nitrogen atmosphere to UV light from a 500-W super-high-pressure mercury lamp for 10 days. The dark blue precipitate (**2**) produced during the photolysis was removed by filtration, and the filtrate was diluted with water (90 mL) and heated at 50 °C for 1 h. Formamidine hydrochloride (2.6 g, 32.3 mmol) was added, and the resulting solution was kept at 4 °C for one week. Brown crystals of **1** (0.319 g) were produced, which were collected by filtration, washed with cold water, and dried in the air; the yield was 18% based on Mo. The above dark blue precipitate (**2**) was washed with ethanol and diethyl ether and dried in the air to yield 0.734 g. The photolysis of **2** in the presence of $C_2H_5CO_2H$ also generated **1**: $C_2H_5CO_2H$ (1.5 mL, 20 mmol) was added to a dark blue solution of **2** (0.25 g) in 8.5 mL of water, and the solution pH level was adjusted to 3.9−4.1 with $NH_4OH$. The UV-photolysis of the resulting solution under the same procedure generated **1** (with the yield of 0.08 g). In the course of our trial to characterize the structure of **2**, $LaCl_3\cdot 7H_2O$ (0.03 g, 0.08 mmol) was added to the solution of **2** (0.1 g) in water (20 mL) and stirred until perfect dissolution. When the resulting solution was kept at 4 °C for one week, blue hexagonal crystals of **3** were produced. The crystals were washed with cold water and dried in the air to yield 0.09 g. Anal. Calcd (Found) for **1**: C, 7.71 (7.70); H, 2.43 (2.43); N, 4.56 (4.57); Mo, 51.5 (52.0). For **3**: Mo, 52.8 (52.0); La, 6.38 (6.29). The manganometric redox titration for **1** and **3** showed the presence of 60 ± 1 and 21 ± 1 $Mo^{V}$ centers, respectively. Selected IR data (KBr pellet, in cm$^{-1}$) for **1**: 1716(s, $\nu_{as}$(C=N)), 1625(w, $\delta(H_2O)$), 1542(m, $\nu_{as}$(COO)), 1424(m), 1400(m, $\delta$ $(NH_4^+)/\nu_s$(COO)), 1083(w), 971(m, $\nu$(Mo=O)), 852(m), 789(s), 721(s), 631(w), 564(m), 460(w), 440(w). For **2**: 1624(m, $\delta(H_2O)$), 1541(m, $\nu_{as}$(COO)), 1401(s, $\delta(NH_4^+)/\nu_s$(COO)), 1296(w), 1084(w), 963(s, $\nu$(Mo=O)), 793(s), 730(m), 647(m), 556(s), 482(w), 430(w). For **3**: 1617(m, $\delta(H_2O)$), 976(s, $\nu$(Mo=O)), 800(s), 720(m), 650(s), 560(s). Together with the results of the X-ray crystallographic analysis; the elemental analysis; and UV/vis absorption, IR, and $^{13}$C NMR spectrometries, **1** and **3** were formulated as given by the above formulas.

**X-Ray Crystallography.** Crystal data of **1** at 173 K: $C_{158}H_{592}N_{80}O_{520}Mo_{132}$, MW = 24 598.72, space group $R\bar{3}$(h) (No. 148), $a$ = 32.93(2), $b$ = 32.93(2), $c$ = 74.5(2) Å, $\alpha$ = 90, $\beta$ = 90, $\gamma$ = 120°, $Z$ = 3, $V$ = 70 021.8 (18) Å$^3$, $\rho$ = 1.792 g cm$^{-3}$, $\mu$ = 18.25 cm$^{-1}$, $F(000)$ = 35 412. A crystal (size = 0.28 × 0.23 × 0.17 mm) of **1** was sealed in a Lindemann glass capillary and mounted on the diffractometer. Intensity data for the single-crystal X-ray crystallography of **1** was measured on a *Saturn* CCD Rigaku diffractometer with graphite monochromatized Mo Kα radiation (= 0.7107 Å) at 173 K. Data collection proceeded by using $\omega$-scan at a 0.5° scan and $\chi$ = 45° in eight runs (with 360 frames respectively) of $-110.0° < \omega < +70.0°$, $\phi$ = 0°; $-110.0° < \omega < +70.0°$, $\phi$ = 90°; $-110.0° < \omega < +70.0°$, $\phi$ = 180°; $-110.0° < \omega < +70.0°$, $\phi$ = 270°; $-125.0° < \omega < +55.0°$, $\phi$ = 0°; $-125.0° < \omega < +55.0°$, $\phi$ = 90°; $-125.0° < \omega < +55.0°$, $\phi$ = 180°; and $-125.0° < \omega < +55.0°$, $\phi$ = 270°. The crystal-to-detector distance was 100 mm. The exposure rate was 20 s/deg. The detector swing angle for the former four runs was −19.82° and for latter four was 34.82°. A total of 532 964 reflections ($0.8° < \theta < 27.9°$) were collected, of which 35 413 unique reflections ($R_{int}$ = 0.111) were used. The structure was solved by a direct method (SHELXS-97) and refined by using the CrystalStructure software package (CRYSTALS) based on 11 095 observed reflections with $I > 2\sigma(I)$ and 665 parameters to $R_1$ = 0.142 and $R_w$ = 0.233 (refined against $|F|$). The highest residual electron density was 2.81 e Å$^{-3}$ at 0.06 Å from the Mo20 atom (the deepest hole, −1.69 e Å$^{-3}$ at 1.52 Å from O1). Lorentz polarization effects and numerical absorption corrections (by using the program Numabs and Shape: Higashi, T. *Program for Absorption Correction*; Rigaku Corporation: Tokyo, 1999) were applied to the intensity data, and H atoms were not indicated in the calculation. Transmission factors were 0.730−0.733. All of the Mo atoms for the anion were refined anisotropically, and all of the O and C atoms for the anion were refined isotropically due to the unstability of their anisotropic refinements. The atoms outside the anion cluster were refined isotropically. It was extremely difficult to distinguish $NH_4^+$ cations from water molecules of crystallization, and not all positions of cations and crystal water molecules in the crystal lattice were located due to disorder. Thus, three N atoms (N1−N3) and two C atoms (C23 and C24) for the cations were refined, and other atoms were refined by using the scattering factor of a neutral oxygen atom (for O85−O105 atoms).

Crystal data of **3** at 100 K: $H_{273}Mo_{96}La_8O_{426.5}$, MW = 17420.38, space group $C2/c$ (No. 15), $a$ = 29.249(7), $b$ = 59.843(15), $c$ = 26.252(6) Å, $\beta$ = 97.935(6)°, $Z$ = 4, $V$ = 45510(20) Å$^3$, $\rho$ = 2.47 g cm$^{-3}$, $\mu$ = 32.77 cm$^{-1}$, $F(000)$ = 32 692. Crystal size = 0.20 × 0.06 × 0.06 mm. The crystal was coated with paraffin oil and mounted in a loop. Intensity data were measured on a Saturn 70VT CCD Rigaku diffractometer with graphite monochromatized Mo Kα radiation (= 0.71071 Å) at 100 K. Data collection proceeded by using $\omega$-scan at a 0.5° scan and $\chi$ = 45° in eight runs (with 360 frames respectively) of $-90.0° < \omega < +90.0°$, $\phi$ = 0°; $-90.0° < \omega < +90.0°$, $\phi$ = 90°; $-90.0° < \omega < +90.0°$, $\phi$ = 180°; $-90.0° < \omega < +90.0°$, $\phi$ = 270°; $-60.0° < \omega < +120.0°$, $\phi$ = 0°; $-60.0° < \omega < +120.0°$, $\phi$ = 90°; $-60.0° < \omega < +120.0°$, $\phi$ = 180°; and $-60.0° < \omega < +120.0°$, $\phi$ = 270°. The crystal-to-detector distance was 80 mm. The exposure rate was 90 s/deg. The detector

(15) Müller, A.; Shah, S. Q. N.; Bögge, H.; Schmidtmann, M.; Kögerler, P.; Hauptfleisch, B.; Leidung, S.; Wittler, K. *Angew. Chem., Int. Ed.* **2000**, *39*, 1614.

swing angle for the former four runs was −0.18° and for the latter four was 29.82°. A total of 290 266 reflections ($0.7° < \theta < 28.5°$) were collected, of which 52 754 unique reflections ($R_{int} = 0.145$) were used. The structure was solved by a direct method (SHELXS-97) and refined by using the CrystalStructure software package (CRYSTALS) based on 13 821 observed reflections with $I > 2.2\sigma(I)$ and 1383 parameters to $R_1 = 0.169$ and $R_w = 0.286$ (refined against $|F^2|$). The highest residual electron density was 5.65 e Å$^{-3}$ at 0.05 Å from the La3 atom (the deepest hole, −3.72 e Å$^{-3}$ at 1.18 Å from La1). Lorentz polarization effects and numerical absorption corrections (by using the program Numabs and Shape: Higashi, T. *Program for Absorption Correction*; Rigaku Corporation: Tokyo, 1999) were applied to the intensity data, and H atoms were not indicated in the calculation. Transmission factors were 0.814−0.821. All of the Mo and La atoms were refined anisotropically. O atoms were refined isotropically, and site occupancies of O200−O230 atoms of the crystal water molecules (O188−O230) were set to be 1/2 through the refinement of their thermal parameters due to disorder. The overall charge of −22 was neutralized with the corresponding number of protons. The number of independent Mo and La atoms in the crystal of **3** is approximately tripled compared with the one in the crystal of **1**, indicating the requirement of significant numbers of the reflections at higher $\theta$ values for **3**. A total of 13 067 unique reflections measured at $\theta$ values higher than 25° help the refinement provide the structure. Tables S1 and S2 (Supporting Information) list the Mo−O bond distances and the interatomic distances of selected atoms for **1** and **3**, respectively. Further details on the crystal structure investigations may be obtained from the Cambridge Crystallographic Data Center (CCDC), e-mail: deposit@ccdc.cam.ac.uk, on quoting the depository numbers CCDC-776972 ($[HC(NH_2)_2]_{26}(NH_4)_{28}[Mo^V_{60}Mo^{VI}_{72}O_{372}(H_2O)_{48}(C_2H_5CO_2)_{36}(^iC_3H_7CO_2)_6]\cdot 16H_2O$ (**1**)) and CCDC-776973 ($H_{22}[Mo^V_{20}Mo^{VI}_{76}O_{301}(H_2O)_{29}\{La(H_2O)_6\}_2\{La(H_2O)_5\}_6]\cdot 54.5H_2O$ (= $\{Mo_{96}La_8\}$) (**3**)).

**Physical Measurements.** IR (as KBr pellet) and UV/vis absorption spectra were recorded on Jasco FT-IR 5000 and Jasco V-570 UV−vis−NIR spectrometers, respectively. UV/vis absorption spectra of the photolyte of each stage of the photolysis were measured by using a quartz cell with an optical length of 0.1 mm or 10 mm without dilution. The contents of Mo and La were determined by inductively coupled plasma atomic emission spectroscopy (ICP) on a Rigaku Spectro CIROS$^{CCD}$ spectrometer.

$^{13}$C NMR spectra of **1** and **2** in $D_2O$ were measured at 297 ± 1 K using Φ = 10-mm-internal-diameter NMR tubes on a JEOL AL-300 spectrometer at 75.6 MHz with 90° pulses. A scan repetition time of 10 s was used, and a line-broadening factor of 0.1 Hz was applied before FT treatment. Chemical shifts were referenced to an external $Na_2CO_3$ solution (1 M in $D_2O$) for which the resonance was taken as $\delta = 0$ ppm.

Electrospray mass spectrometry (ESI-MS) measurements were recorded by using an ion trap mass spectrometer (Bruker Daltonics microTOF) equipped with an electrospray ionization (ESI) source operated in negative-ion mode.[1c,8] The tip of the capillary and the capillary exit were maintained at potentials of 3.5 kV and −80 V, respectively, relative to the ground. The source temperature was 160 °C. Sample solutions (2−30 μM of **1** or 1−10 mg in 20 mL for **2**) in water and $10^3$-fold dilution of photolytes by water were infused by using a syringe pump into the ESI source at a flow rate of 500 μL h$^{-1}$.

## Results

**Formation of {Mo$_{132}$} Keplerate through Mo-blue Intermediate.** The complex obtained by the prolonged UV-photolysis of the $\{Mo^{VI}_7\}/C_2H_5CO_2H$ system at pH 3.9−4.1, $[HC(NH_2)_2]_{26}(NH_4)_{28}[Mo^V_{60}Mo^{VI}_{72}O_{372}(H_2O)_{48}(C_2H_5CO_2)_{36}(^iC_3H_7CO_2)_6]\cdot 16H_2O$ (**1**), is the formamidinium/ammonium-mixed salt of carboxylate-coordinated $\{Mo_{132}\}$ Keplerate (**1a**). Compound **1a** consists of 12 $\{(Mo^{VI})(Mo^{VI}_5)\}$ pentagonal subunits and 30 $\{Mo^V_2\}$ linkers,[12,13] and each of them exhibits a bidentate mode of coordination of $C_2H_5CO_2^-$ and $^iC_3H_7CO_2^-$ to give the formula of **1a**, $\{[(Mo^{VI})Mo^{VI}_5O_{21}(H_2O)_4(C_2H_5CO_2)]_{12}[Mo^V_2O_4(C_2H_5CO_2)]_{24}[Mo^V_2O_4(^iC_3H_7CO_2)]_6\}^{54-} \equiv [\{[(Mo^{VI})Mo^{VI}_5O_{21}(H_2O)_4(C_2H_5CO_2)][Mo^VO_2(0.4C_2H_5CO_2 + 0.1\,^iC_3H_7CO_2)]_5\}_{12}]^{54-}$. Compound **1a** is the first Keplerate anion, in which carboxylates are coordinated to both $\{(Mo^{VI})(Mo^{VI}_5)\}$ and $\{Mo^V_2\}$: although the ball-structural complex coordinating the carboxylates to the pentagonal subunits enables exemplification by $\{[(Mo)Mo_5O_{21}(H_2O)_4(CH_3CO_2)]_{12}[Mo^VO(H_2O)]_{30}\}$,[15] this complex is a neutral cluster with a blue color due to a partial reduction of 12 $\{(Mo^{VI})(Mo^{VI}_5)\}$ pentagonal subunits with a subsequent magnetic coupling with $[Mo^VO(H_2O)]^{3+}$ linkers, which was prepared by the oxidation of $\{[(Mo^{VI})Mo^{VI}_5O_{21}(H_2O)_6]_{12}[Mo^V_2O_4(CH_3CO_2)]_{30}\}^{12-}$ in water under air. Figure 2 shows the structure (a) and the asymmetric fragment (b) of **1a**. In an asymmetric unit (corresponding to 1/6 anion) for **1a**, $\{[(Mo^{VI})Mo^{VI}_5O_{21}(H_2O)_4(C_2H_5CO_2)]_2[Mo^V_2O_4(0.8C_2H_5CO_2 + 0.2\,^iC_3H_7CO_2)]_5\}^{9-}$, one of five $[Mo^V_2O_4(\text{carboxylate})]^+$ (= $\{Mo^V_2(\text{carboxylate})\}$) linkers comprises $^iC_3H_7CO_2^-$ (isobutyrate, one of the photoproducts) instead of $C_2H_5CO_2^-$ (Figure 2b). The coordination of the photo-oxidation product has also been reported for $\{Mo_{142}(CH_3CO_2)_5(C_2H_5CO_2)\}$ produced by the UV-photolysis of the $\{Mo^{VI}_7\}/CH_3CO_2H$ system at pH 3.4, where the coordination ratio of acetate to propionate is 5:1.[7] As well as other Keplerate ions, **1a** constructs 20 $\{Mo_9O_9\}$ pores (with about 6.6 Å size) involving three diamagnetic $Mo^V-Mo^V$ dumbbells (of $Mo^V-Mo^V$ bonds at 2.6 Å in the $[Mo^V_2O_4(\text{carboxylate})]^+$ linker) and three $Mo^{VI}$ sites (of the pentagonal subunit peripheries).[15,16]

It is noteworthy that the formation of **1a** at pH 3.9−4.1 was always preceded by the precipitation of the dark blue Mo-blue precursor (**2**) through more than 2 days of photolysis and that the UV photolysis of **2** in the presence of $C_2H_5CO_2H$ at pH 3.9−4.1 is essential for the formation of **1a**. Figure 3 shows electronic absorption spectra of **1** (a) and **2** (b) and the UV-photolysis (c) of **2** to **1a** in water at pH 4. In Figure 3a and b, the spectra of 12-e$^-$-reduced $\{Mo_{16}\}$ (at pH 5.4)[1c] and 28-e$^-$-reduced $\{Mo_{142}(CH_3CO_2)_5(C_2H_5CO_2)\}$ (at pH 3.4)[7] are added for comparison, respectively. Compound **1a** at pH 4 shows an absorption maximum due to 30 $Mo^V-Mo^V$ bonds around 456 nm with $\varepsilon_{456} = 2.5 \times 10^5$ M$^{-1}$ cm$^{-1}$ of the molecular absorption coefficient, which is much (approximately 100-fold) larger than the $\varepsilon_{380} = 2.3 \times 10^3$ M$^{-1}$ cm$^{-1}$ for $\{Mo_{16}\}$, showing weak shoulder peaks due to six $Mo^V-Mo^V$ bonds with a 2.6 Å distance in the ε-Keggin structure. Since the reddish-brown color is attributed to the electronic transition of $[(d_{xy}{}^A + d_{xy}{}^B)/\sqrt{2}] \rightarrow [(d_{xy}{}^A - d_{xy}{}^B)/\sqrt{2}]$ for the localized $Mo^V{}_A-Mo^V{}_B$ bond as discussed for $\{Mo_{16}\}$,[1c] a large value of $\varepsilon_{456}$ for **1** is associated

(16) (a) Mitra, T.; Tomsa, A.-R.; Merca, A.; Bögge, H.; Avalos, J. B.; Poblet, J. M.; Bo, C.; Müller, A. *Chem.—Eur. J.* **2009**, *15*, 1844. (b) Müller, A.; Das, S. K.; Talismanov, S.; Roy, S.; Beckmann, E.; Bögge, H.; Schmidtmann, M.; Merca, A.; Berkle, A.; Allouche, L.; Zhou, Y.; Zhang, L. *Angew. Chem., Int. Ed.* **2003**, *42*, 5039. (c) Müller, A.; Krickenmeyer, E.; Bögge, H.; Schmidtmann, M.; Roy, S.; Berkle, A. *Angew. Chem.* **2002**, *114*, 3756.

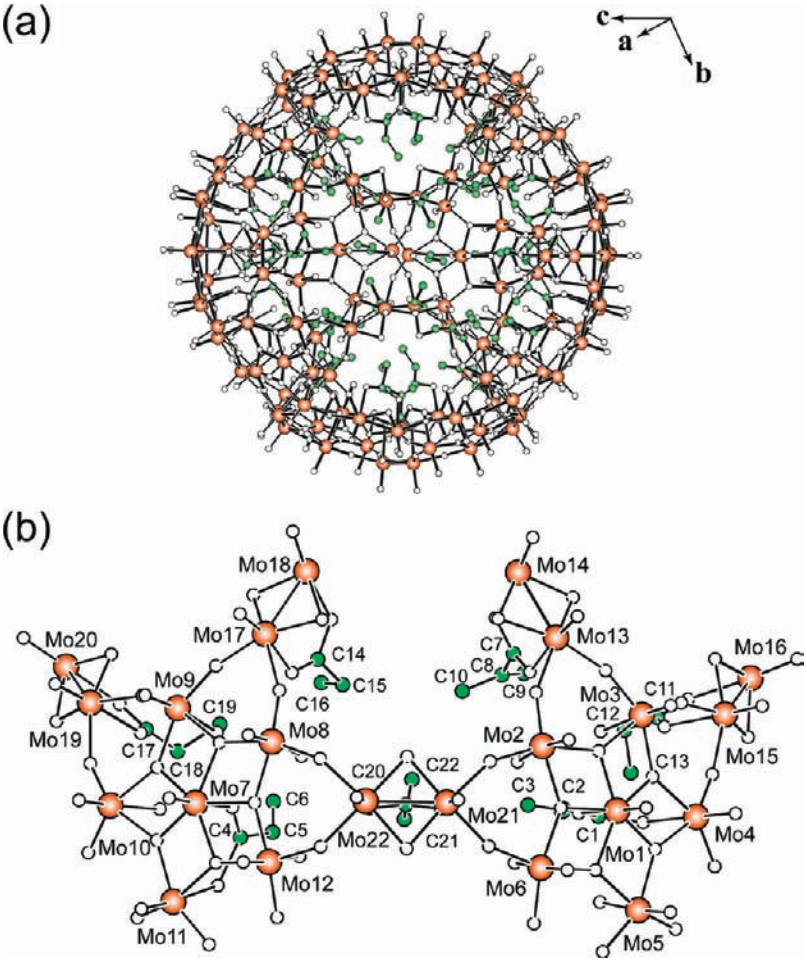


**Figure 2.** Structure (a) and asymmetric unit (b) of $\{[(Mo^{VI})Mo^{VI}_5O_{21}(H_2O)_4(C_2H_5CO_2)]_2[Mo^{V}_2O_4(0.8C_2H_5CO_2 + 0.2^{i}C_3H_7CO_2)]_5\}^{9-}$ (**1a**).

with a small distortion of the $Mo^{V}O_6$ octahedra involved in the $Mo^{V}-Mo^{V}$ bonds compared with $\{Mo_{16}\}$, as shown in the inset of Figure 3a, where the selected *trans* $O-Mo^{V}-O$ and $O-Mo^{V}-Mo^{V}$ bond angles for the $Mo^{V}O_6$ octahedra are compared between **1** and $\{Mo_{16}\}$. The UV/vis absorption spectrum of **2** shows the absorption maxima around 740 and 1100 nm (at pH 4.6) and is similar to that of $\{Mo_{142}(CH_3CO_2)_5(C_2H_5CO_2)\}$.[7] UV-photolysis of the aqueous solution containing **2** (0.25 g in 10 mL) and $C_2H_5CO_2H$ (of 2.0 M) at pH 4 reveals the formation of **1a** as supported by the observation of the absorption around $\lambda_{max}$ = 456 nm (Figure 3c). Figure 4 shows IR spectra of **1** and **2** together with the spectra of $\{Mo_{142}\}$[1a] and $\{Mo_{142}(CH_3CO_2)_5(C_2H_5CO_2)\}$[7] for comparison. IR spectra of **1**, **2**, and $\{Mo_{142}(CH_3CO_2)_5(C_2H_5CO_2)\}$ resemble each other in the range 1300−1700 $cm^{-1}$, and they show $\delta(H_2O)$ around 1625 $cm^{-1}$ and $\delta$(COO) around 1541 and 1400 $cm^{-1}$ in contrast to the observation of the weak intensity around 1400−1550 $cm^{-1}$ for $\{Mo_{142}\}$. Together with the similarity of the electronic absorption spectra between **2** and $\{Mo_{142}(CH_3CO_2)_5(C_2H_5CO_2)\}$ (Figure 3b), **2** is suggested to be the carboxylate-coodinated Mo-blue ring species. The coordination of carboxylates in **2** was supported by the $^{13}C$ NMR spectrum of **2** recorded at room temperature in $D_2O$ (Figure S1, Supporting Information), which exhibits three singlet lines around $\delta$ = +12, −140, and −159 ppm due to $CH_3-$, $-CH_2-$, and $-CO_2^-$− carbon atoms of propionate, respectively. Either line of the observable two lines around $\delta$ = −159 ppm could be attributed to the propionate released partially from the parent anion through the exchange with $D_2O$ molecules. Similarly, the observable two singlet lines around $\delta$ = −11 ppm due to the formamidium carbon atom on the $^{13}C$ NMR spectrum of **1** (Figure S1) were attributed to the electrostatic interaction with the carboxylate released partially from **1a** through the exchange with $D_2O$ molecules. The expected intensity of the *iso*-butyrate carbon atoms was too weak to be detected on $^{13}C$ NMR spectra of **1** and **2**.

**{$Mo_{96}La_8$} Eggshell Ring Chain.** The addition of $La^{3+}$ to an aqueous solution of **2** at 4 °C generates chain-structural hexagon-shaped crystals of the novel eggshell rings formulated by $H_{22}[Mo^{V}_{20}Mo^{VI}_{76}O_{301}(H_2O)_{29}\{La(H_2O)_6\}_2\{La(H_2O)_5\}_6]\cdot 54.5H_2O$ (= $\{Mo_{96}La_8\}$) (**3**). The IR spectrum of **3** is shown in comparison with that of **2** in Figure S2 (Supporting Information), where no observation of $\delta$(COO) around 1400−1550 $cm^{-1}$ for **3** implies a facile removal of the coordinated carboxylates from **2** through the reaction with $La^{3+}$. There being no observable location of La atoms outside the cluster anion (**3a**) with the use of X-ray diffraction allows us to formulate **3** as a $H^+$ salt, along with the results of the elemental analysis and the IR spectrometry. The UV/vis absorption spectrum of **3** showed two absorption maxima around 760 and 1120 nm with $\varepsilon_{760}$ = $5.3 \times 10^4$ and $\varepsilon_{1120}$ = $3.8 \times 10^4$ $M^{-1}$ $cm^{-1}$ in aqueous solutions, which was similar to **2**.

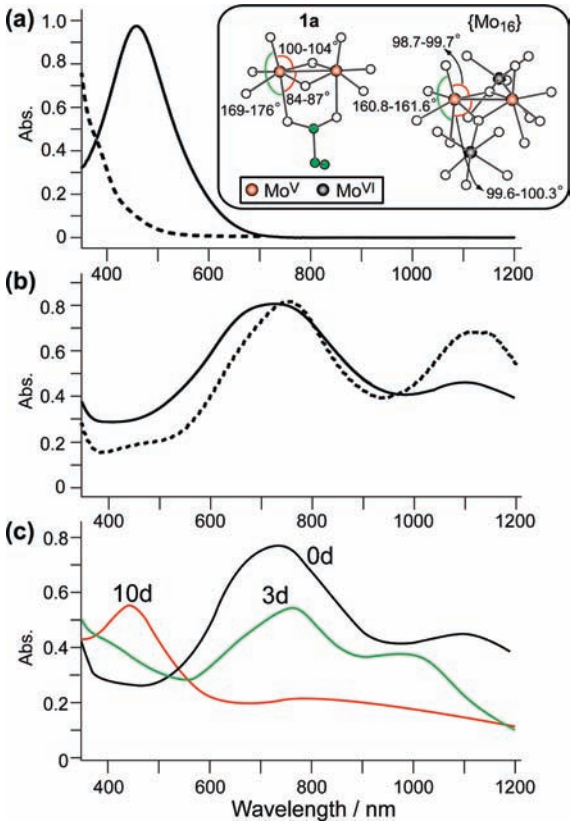


**Figure 3.** Electronic absorption spectra of **1** (4.0 $\mu$M, a), **2** (5 mg in 20 mL water, b), and photolytes (0-, 3-, and 9-day photolyses) of the **2** (0.25 g in 10 mL water)/$C_2H_5CO_2H$ (2.0 M) system at pH 4 (c). Dotted lines in a and b indicate the spectra of $\{Mo_{16}\}$ (0.17 mM at pH 5.4) and $\{Mo_{142}(CH_3CO_2)_5(C_2H_5CO_2)\}$ (6.2 $\mu$M at pH 3.4), respectively. The inset figure in a indicates selected O−$Mo^V$−O and O−$Mo^V$−$Mo^V$ bond angles for the $Mo^VO_6$ octahedra of **1** and $\{Mo_{16}\}$: *trans* O−$Mo^V$−O bond angles of 169−176° and O−$Mo^V$−$Mo^V$ bond angles of 84−87° and 100−104° for **1** and 160.8−161.6° and 98.7−99.7° and 99.6−100.3° for $\{Mo_{16}\}$. The spectra in a, b, and c are measured with optical path-length cells of 10, 10, and 0.1 mm, respectively.

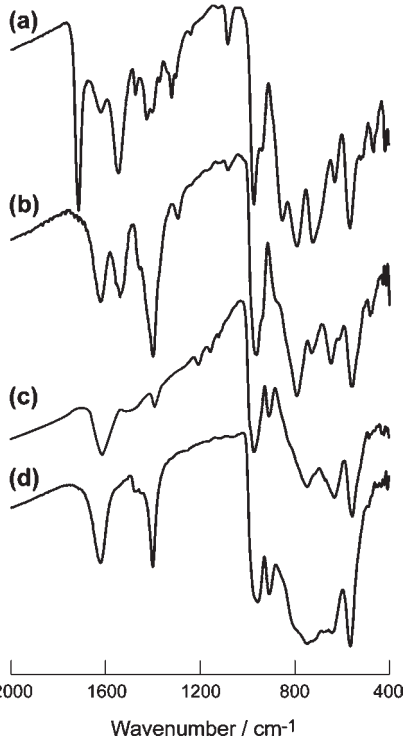


**Figure 4.** IR spectra of **1** (a), **2** (b), $\{Mo_{142}\}$ (c),[1a] and $\{Mo_{142}(CH_3CO_2)_5(C_2H_5CO_2)\}$ (d).[7]

Figure 5 shows structures of the asymmetric unit (a) corresponding to a half anion with the indication of six types of Mo atoms discriminated by different colors, the eggshell ring (b) with outer-ring diameters of approximately 2.7 and 2.4 nm and inner-ring diameters of approximately 1.5 and 1.1 nm for the 20-$e^-$-reduced **3a**, and the linkage between the rings through the Mo−O−Mo bonds in the lattice (c). Figure 5b also shows Mo−O−Mo and O−Mo−O bond angles ($\omega_1$, $\omega_2$, and $\omega_3$) and Mo−O bond distances ($l_1$ and $l_2$) at the −O−Mo−O−Mo−O− linkage within the equator outer ring for the estimation of the molecular curvature of **3a**.[1a,7,17] The structure of each eggshell ring exhibits the $C_2$ local symmetry and comprises one binuclear (Mo40 and 40′) "spacer" in the outer ring and two sets of the binuclear (Mo2 and 48) linker and four $La^{3+}$ (La1− La4) atoms in the inner rings, where the primed (′) atom means the atom related by $(1 - x, y, 1/2 - z)$ symmetry. Figure 6 shows the structure of the environment of the spacer with the selected atomic distances (in Å). The eggshell ring structure results from the insertion of $[Mo^{VI}_2O_7(H_2O)]^{2-}$ (=$\{Mo^{VI}_2\}$ spacer) into the equator outer ring of the hypothetical $\{Mo_{94}La_8\}$ ring predicted by the pinning between *shoulder* and *equator* Mo atoms through the Mo5−O166′−Mo46′ (and Mo5′−O166−Mo46) bond instead of the Mo5−O140−Mo40 bond (at 1.82 and 1.95 Å for Mo5−O140 and Mo40−O140 bond lengths, respectively). There being no X-ray crystallographic indication of the coordination of the aqua molecule to the *shoulder* Mo5 (or Mo5′) atom is different from the cases of discrete Mo-blue rings generated by the dehydrative condensations of four-$e^-$-reduced $\{Mo_{20}\}$/$\{Mo_{21}\}$/$\{Mo_{22}\}$ building blocks which provided the coordination of one aqua ligand to each of all *linker*, *head*, and *shoulder* Mo atoms.[1a,2−7] Both O55 (as aqua O atom) and O142 atoms in the binuclear spacer are positioned on the molecular $C_2$ axis and link the two *spacer* Mo40 atoms (of edge-shared $MoO_6$ octahedra) at a Mo···Mo′ distance of 3.39 Å. Figure 7 shows the structure of the environment of the binuclear linker with selected Mo−O atomic distances (in Å). Although the *linker* Mo2 (or Mo48) atom of the binuclear linker remaining in the half anion is connected with both the *head* and *shoulder* Mo atoms of Mo37 and Mo43 (Mo45 and Mo1) through the Mo−O−Mo bonds in the same mode as for the other Mo-blue rings,[1a,2−7] neither the Mo2 nor the Mo48 atom coordinates the aqua ligand in contrast to the $\{Mo^{VI}_2\}$ linkers in the discrete Mo-blue rings. Since the $\{Mo_{96}La_8\}$ eggshell ring comprises 10 *head*, 20 *shoulder*, and two *spacer* Mo atoms, the number of aqua ligands coordinated to Mo atoms for each ring in **3a** is estimated to be 29 (=10 + 18 + 1). As shown in Figure 7, the *linker* Mo48 atom is surrounded by five O (54, 109, 134, 181, and 183) atoms at Mo−O distances of 1.70−2.19 Å, whereas another *linker* Mo2 atom coordinates six O (52, 85, 109, 133, 151, and 179) atoms at Mo−O distances of 1.70−2.08 Å. The long distance (of 2.81 Å) between Mo48 and

(17) Yamase, T.; Ishikawa, E.; Abe, Y.; Yano, Y. *J. Alloys Compd.* **2006**, *408*−*412*, 693.

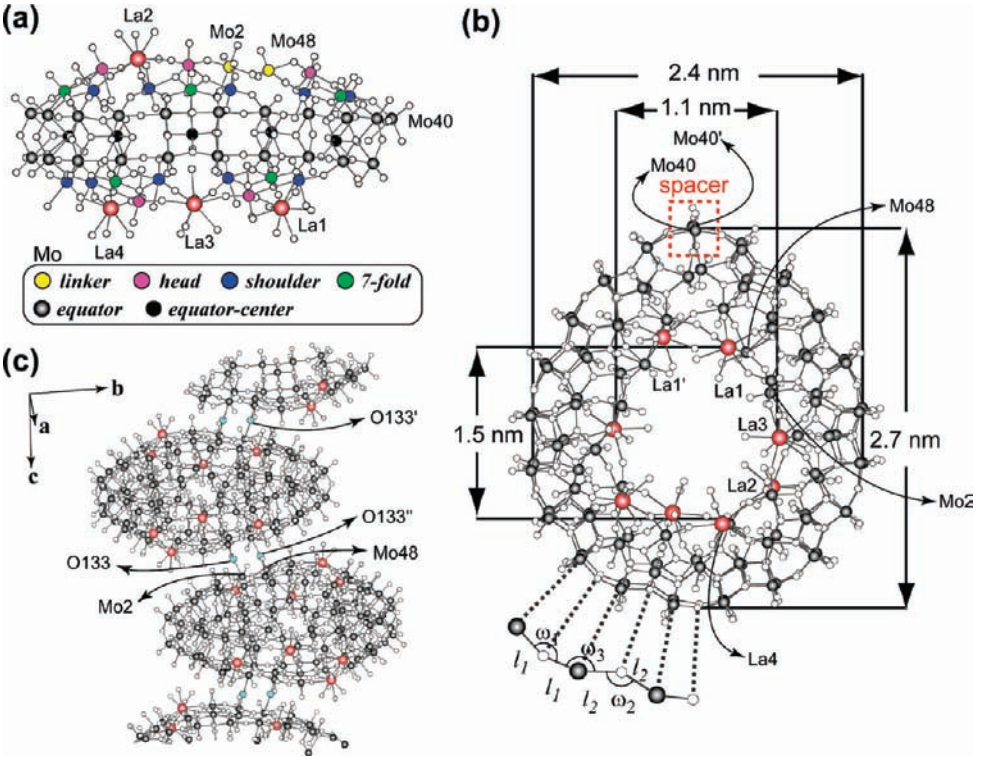


**Figure 5.** Structures of the asymmetric unit (a), and the eggshell ring (b) for the $\{Mo_{96}La_8\}$ anion (**3a**), and the chain through the linkage among the rings in the lattice (c). Six types (*linker*, *head*, *shoulder*, *7-fold*, *equator*, and *equator-center*) of Mo atoms in a are indicated by different colored balls for clarification.

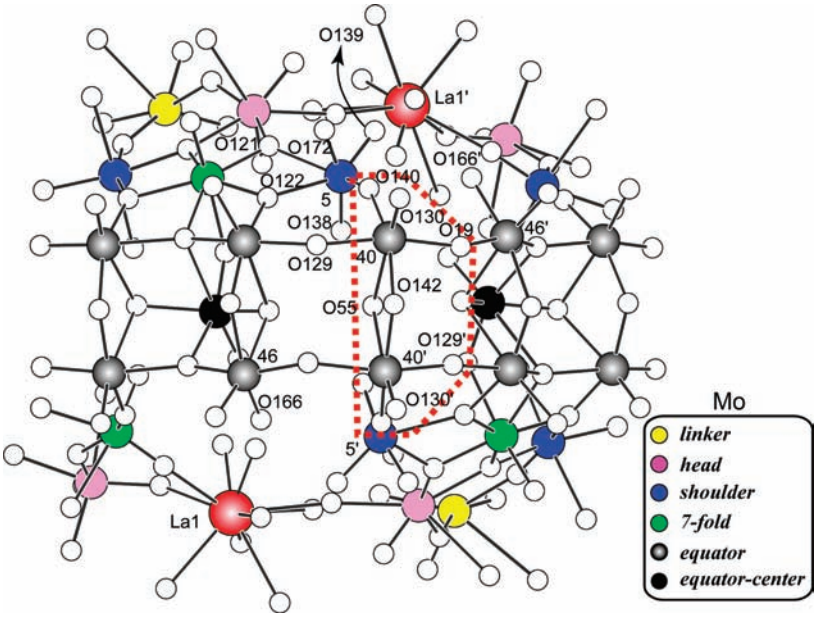


**Figure 6.** Structure of the environment of the "spacer" with selected atomic distances (in Å): Mo40−O19, 1.97(4); Mo40−O55, 2.42(3); Mo40−O129, 1.86(5); Mo40−O130, 1.64(4); Mo40−O140, 1.95(4); Mo40−O142, 1.87(2); Mo40···Mo40′, 3.391(10); Mo5−O121, 2.16(4); Mo5−O122, 2,21(4); Mo5−O138, 1.74(6); Mo5−O139, 1.65(8); Mo5−O140, 1.82(4); Mo5−O172, 1.46(3). The part surrounded by the red-colored dotted line indicates $[Mo^{VI}_2O_7(H_2O)]^{2-}$ (= $\{Mo^{VI}_2\}$ spacer), in which the aqua O atom is O55. The primed (′) atom means the atom related by $(1 - x, y, 1/2 - z)$ symmetry. Six types (*linker*, *head*, *shoulder*, *7-fold*, *equator*, and *equator-center*) of Mo atoms are indicated by different colored balls for clarification.

O133″ atoms (where the doubly primed atom belongs to the neighboring eggshell ring related by $(3/2 - x, 1/2 - y, 1 - z)$ symmetry) lets us conceive of the binding between the two atoms with a resultant 6-fold coordination of the *linker* Mo48 atom. Such a coordination motif for the *linker* Mo48 atom leads to the chain structure with Mo48−O133″−Mo2″ and Mo2−O133−Mo48″ linkages between the two binuclear $[Mo^{VI}_2O_6]$ linkers of neighboring molecules for **3a** (Figure 5c).

Four La atoms (La1−La4) in the half ring show the distorted tricapped-trigonal-prismatic $LaO_9$ coordination geometries (at La−O distances of 2.3−2.9 Å), which

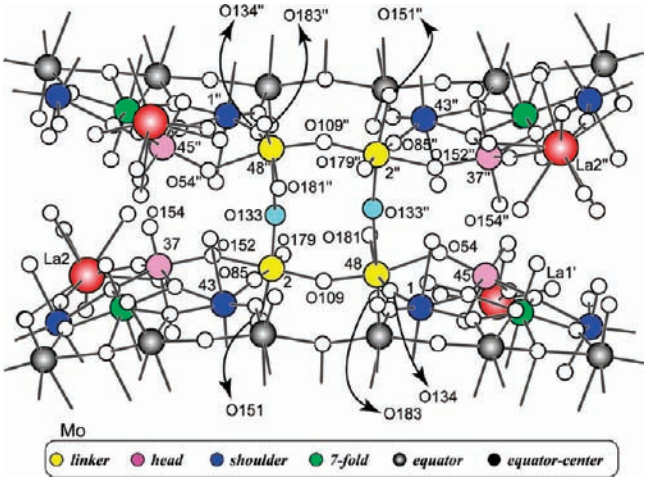


**Figure 7.** Structure of the environment of the binuclear linker with selected Mo−O atomic distances (in Å): Mo2−O85, 2.08(3); Mo2−O109, 1.87(3); Mo2−O133, 1.85(6); Mo2−O151, 1.99(5); Mo2−O152, 1.97(3); Mo2−O179, 1.70(5), Mo48−O54, 2.19(6); Mo48−O109, 1.87(4); Mo48−O133″, 2.81(6); Mo48−O134, 2.06(5); Mo48−O181, 1.70(7); Mo48−O183, 1.97(11). The doubly primed (″) atom means the atom related by (3/2 − *x*, 1/2 − *y*, 1 − *z*) symmetry. Six types (*linker*, *head*, *shoulder*, *7-fold*, *equator*, and *equator-center*) of Mo atoms are indicated by different colored balls for clarification.

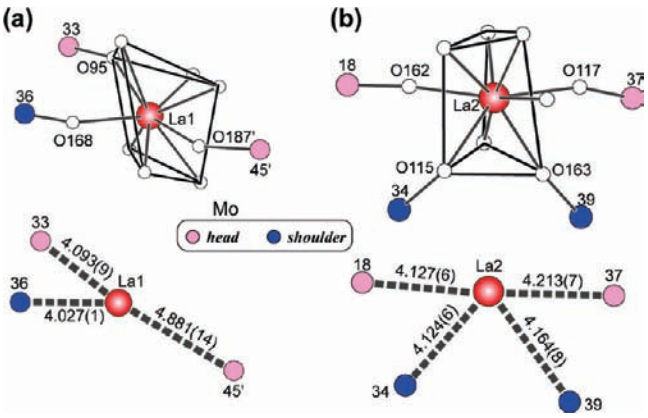


**Figure 8.** The distorted tricapped-trigonal-prismatic coordination geometries of both $LaO_3(H_2O)_6$ for the La1 atom (a) and $LaO_4(H_2O)_5$ for La2 (b) with Mo−O, La−O, and La···Mo atomic distances (in Å): Mo18−O162, 1.75(3); Mo33−O95, 1.77(3); Mo34−O115, 1.67(3); Mo36−O168, 1.56(5); Mo37−O117, 1.61(4); Mo39−O163, 1.67(4); Mo45′−O187′, 2.23(8); La1−O95, 2.54(3); La1−O168, 2.51(5); La1−O187′, 2.81(8); La2−O115, 2.53(3); La2−O117, 2.65(4); La2−O162, 2.48(3); La2−O163, 2.54(4). The primed (′) atom means the atom related by (1 − *x*, *y*, 1/2 − *z*) symmetry. Two types (*head* and *shoulder*) of Mo atoms are indicated by different colored balls.

are classified into two types of coordination to the inner ring, 3-fold $LaO_3(H_2O)_6$ (for La1 atom) and 4-fold $LaO_4(H_2O)_5$ (for other La atoms). The $LaO_3(H_2O)_6$ geometry comprises O atoms belonging to three $MoO_6$ octahedra at two *head* and one *shoulder* Mo atom, and the $LaO_4(H_2O)_5$ geometry comprises O atoms belonging to four $MoO_6$ octahedra at two *head* and two *shoulder* Mo atoms. Figure 8 exemplifies the coordination geometries of both $LaO_3(H_2O)_6$ for the La1 atom and $LaO_4(H_2O)_5$ for La2. The La1 site shows a significantly long La−O distance of 2.81 Å for the aqua O187′ atom coordinated to the *head* Mo45′ atom at a Mo−O distance of 2.23 Å and also shows 2.54 and 2.51 Å for O95 and O168 atoms coordinated to the *head* Mo33 and *shoulder* Mo36 atoms with Mo−O distances of 1.77 and 1.56 Å, respectively. The La1 site involving the long La−O distance of 2.81 Å is in strong contrast with the other La sites which show La−O distances of 2.4−2.7 Å, as observed also for both Japanese rice-ball-shaped $[Mo^{V}_{24}Mo^{VI}_{96}O_{366}H_{14}(H_2O)_{48}\{La(H_2O)_5\}_6]^{4-}$ (= $\{Mo_{120}(La)_6\}$) and elliptical $[Mo^{V}_{28}Mo^{VI}_{122}O_{452}H_2(H_2O)_{66}\{La(H_2O)_5\}_2]^{24-}$ (= $\{Mo_{150}(La)_2\}$) rings.[17] As a result, the La1 site exhibits asymmetric La···Mo distances (4.9 and 4.0−4.1 Å) for the Mo···La···Mo linkage, while the other La atoms indicate approximately symmetric La···Mo distances of 4.1−4.2 Å for the *head* and *shoulder* Mo atoms. A simplified Mo framework of the $\{Mo_{96}La_8\}$ eggshell ring is shown in Figure 9, where all of the Mo−O−Mo and La−O−Mo bonds in the molecule are depicted by Mo−Mo and La−Mo linkages, respectively. As also shown in Figure 9, the $\{Mo_{96}La_8\}$ ring consists of four$\{Mo_9La\}$, two$\{Mo_{10}La\}$, two$\{Mo_9\}$, and two $\{Mo_{10}La\}$* (as for La1 atom) building subunits and one $\{Mo^{VI}_2\}$ spacer.[18] The insertion of the $\{Mo^{VI}_2\}$ spacer into the outer ring results in the asymmetric 3-fold coordination of the La1 atom (for $\{Mo_{10}La\}$*) in the inner ring, and the *linker* Mo2 and 48 atoms are connected with the *linker* Mo atoms of the neighboring molecules to build the chain structure. The chain structure is associated with the previous finding that the coexistence of $La^{3+}$ in the self-assembly process of the Mo-blue rings not only gives rise to the incorporation of $La^{3+}$ within the inner ring but also provides the Mo-blue ring aggregates due to the dehydrated condensation between the two inner rings of the neighboring Mo-blue rings, as exemplified by the $\{(Mo_{154})_\infty\}$ nanotube.[6a] The chain structure due to a similar linkage between $\{Mo^{VI}_2\}$ linkers of neighbors is known for $\{Mo_{154}\}$ and $\{Mo_{144}\}$, which were prepared thermally for the $Na_2MoO_4$/Fe and $\{Mo^{VI}_7\}$/$Na_2S_2O_4$/$(NH_2)_2CO$ systems around pH = 1 without the help of $La^{3+}$.[19]

**High Nuclearity Mo-blue Ring as an Intermediate.** It has been recently demonstrated that the coordination of $\{Mo_{142}(CH_3CO_2)_5(C_2H_5CO_2)\}$ to $La^{3+}$ generates the elliptical Mo-blue ring, $[Mo^{V}_{28}Mo^{VI}_{106}O_{416}H_{20}(H_2O)_{46}\{La(H_2O)_5\}_4\{La(H_2O)_7\}_4\{LaCl_2(H_2O)_5\}_2]^{10-}$ (=$\{Mo_{134}(La)_{10}\}$), through the superiority of the coordination at the defect pockets to the displacement of the $\{Mo^{VI}_2$(carboxylate)$\}$ linkers.[20] This provides a clue toward the structure of **2** by substituting $La^{3+}$ in **3a** with the defect pocket or $\{Mo^{VI}_2\}$/$\{Mo^{VI}_2$(carboxylate)$\}$ linker. If **2** could be the carboxylate-coordinated Mo-blue ring (as suggested above by IR, UV/vis-absorption, and $^{13}C$ NMR spectrometries), it is reasonable to assume that the $\{Mo^{VI}_2\}$ spacer in **3a** originates from the $\{Mo^{VI}_2\}$/$\{Mo^{VI}_2$(carboxylate)$\}$ linkers in **2** through their displacement with $La^{3+}$. Thus, the anion of **2** could be assigned to the carboxylate-coordinated Mo-blue ring belonging to $\{Mo_{94+2(8-n)}\}$ (*n* is the number of the defect pockets in the molecule) with the

(18) It is possible to say that **3a** consists of two $\{Mo_{18}(La)_2\}$, two $\{Mo_{19}(La)\}$, and one $\{Mo_{22}(La)_2\}$* Mo framework, if we consider that $\{Mo_{22}(La)_2\}$* could be divided into two $\{Mo_{10}(La)\}$* subunit Mo frameworks and one $\{Mo^{VI}_2\}$ spacer.

(19) (a) Müller, A.; Krickemeyer, E.; Bögge, H.; Schmidtmann, M.; Peters, F.; Menke, K; Meyer, J.. *Angew. Chem., Int. Ed.* **1997**, *36*, 484. (b) Müller, A.; Roy, S.; Schmidtmann, M.; Bögge, H. *Chem. Commun.* **2002**, 2000.

(20) Ishikawa, E.; Yano, Y.; Yamase, T. *Materials* **2010**, *3*, 64.

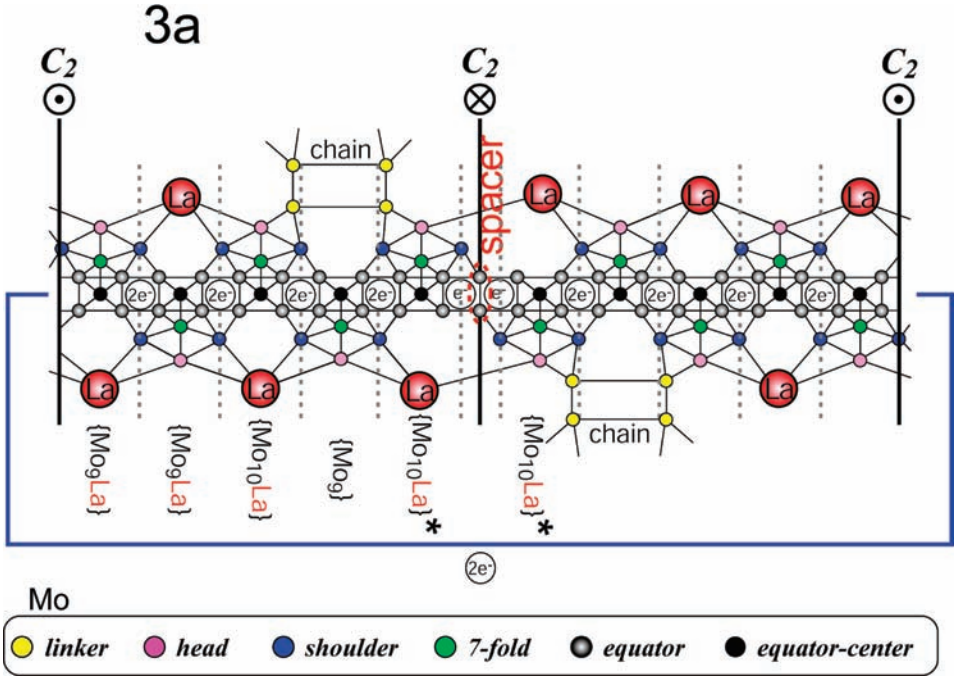


**Figure 9.** Mo framework of the $\{Mo_{96}La_8\}$-blue ring (**3a**) with the location of the $C_2$ axis. The sequence of the subunits for the half ring is $\{Mo_9La\}$, $\{Mo_9La\}$, $\{Mo_{10}La\}$, $\{Mo_9\}$, and $\{Mo_{10}La\}$* from left to right. The $\{Mo^{VI}{}_2\}$ spacer surrounded by the red-colored dotted line is sandwiched by two $\{Mo_{10}La\}$* subunits in the center. Six types (*linker*, *head*, *shoulder*, *7-fold*, *equator*, and *equator-center*) of Mo atoms are indicated by different colored balls for clarification.

molecular weight in the range of 15 194−17 533 (when 0−20 is assumed for the number of the $C_2H_5CO_2^-$ coordination) corresponding to formally five four-e$^-$-reduced building units of $\{Mo_{20}\}$ (= $[Mo^V{}_4Mo^{VI}{}_{16}O_{61}(H_2O)_8]^{6-}$), $\{Mo_{21}\}$ (= $[Mo^V{}_4Mo^{VI}{}_{17}O_{63.5}(H_2O)_9]^{5-}$), and $\{Mo_{22}\}$ (= $[Mo^V{}_4Mo^{VI}{}_{18}O_{66}(H_2O)_{10}]^{4-}$). The result of the manganometric redox titration for **2** (assumed to be the $[NH_4]^+$ salt) gave the presence of 20−24 $Mo^V$ centers for a range of the molecular weight close to the value (= 20) of that for **3**. In addition, the results of both the elemental analysis (C, 2.51; H, 1.85; N, 3.19; Mo, 57.0) and the molecular absorption coefficients estimated for electronic absorption maxima ($\varepsilon_{740} \approx 5 \times 10^4$ and $\varepsilon_{1100} \approx 3 \times 10^4$ $M^{-1}$ $cm^{-1}$ in the same order as for **3**, when the molecular weight at the above range was employed) of **2** go along with the assignment of **2** as a high nuclearity Mo-blue ring species.

The ESI-MS spectrum of the aqueous solution of **2** shows broad signals in the range of $m/z$ 1700−2500 and are unambiguously assigned to charge states of −9,−8, and −7 and correspond to a mass of 15 772.0 ± 10, as shown in Figure 10, where the ESI-MS spectrum of an aqueous solution (at 3−5 $\mu$M) of **1** is shown for comparison. Our investigation of the ESI-MS and CSI-MS spectrometry of $\{Mo_{142}(CH_3CO_2)_5(C_2H_5CO_2)\}$ indicated that the ionization procedure on measurements always brought about the removal of one to four $\{Mo^{VI}{}_2\}$/$\{Mo^{VI}{}_2(carboxylate)\}$ linkers from the Mo-blue ring.[8] Similar behavior has been suggested for the matrix-assisted laser desorption/ionization time-of-flight mass spectrometry (MALDI-TOF-MS) of Mo-blue rings such as $[Mo_{78}Fe_{30}O_{274}(H_2O)_{94}(CH_3CO_2)_{12}]\cdot\sim 150H_2O$,[21a] $[Mo_{102}O_{252}(H_2O)_{78}(CH_3CO_2)_{12}]\cdot\sim 150H_2O$,[21a] and $Na_{32-n}[H_nMo_{176}O_{528}(H_2O)_{63}(CH_3OH)_{17}]\cdot\sim 30H_2O$.[21b] Thus, the estimated mass of 15 772.0 ± 10 for **2** (Figure 10a) would reflect a high nuclearity Mo-blue ring derivative such as $\{Mo_{100}\}$−$\{Mo_{105}\}$ (with the molecular weight corresponding to approximately five $\{Mo_{20}\}$/$\{Mo_{21}\}$ building units) as a result of the partial removal of $\{Mo^{VI}{}_2\}$/$\{Mo^{VI}{}_2(carboxylate)\}$ linkers. The partial removal of the binuclear linkers from the parent molecule on the ESI-MS measurement was suggested also for **1** (Figure 10b): more discrete signals observed in the range of $m/z$ 1600−2400 were unambiguously assigned to charge states of −13, −12, −11, and −10, which correspond to a mass of 21 900 ± 100, on the same order as the mass (fw: 22 630.1) of **1a**. A displacement of the molecular mass from the value expected for **1a** could be tentatively associated with the missing of three or four $[Mo^V{}_2O_4(C_2H_5CO_2)]^+$ (=$\{Mo^V{}_2(carboxylate)\}$) linkers from **1a** to be assigned to $\{[NH_4]_{12}H_{32+x}[Mo^V{}_{54}Mo^{VI}{}_{72}O_{360}(H_2O)_{48}(C_2H_5CO_2)_{33}(^iC_3H_7CO_2)_6]\}^{(13-x)-}$ (fw: 21 888.4, $x$ = 0−3) or $[HC(NH_2)_2]_2[NH_4]_{27}H_{16+x}[Mo^V{}_{52}Mo^{VI}{}_{72}O_{356}(H_2O)_{48}(C_2H_5CO_2)_{32}(^iC_3H_7CO_2)_6]^{(13-x)-}$ (fw: 21 902.6, $x$ = 0−3).

## Discussion

The incorporation of $La^{3+}$ into **2** generates the $\{Mo_{96}La_8\}$ eggshell ring (**3a**; Figure 5). The $\{Mo^{VI}{}_2\}$ spacer (with a Mo···Mo distance of 3.39 Å) in the outer ring of **3a** originates from the $La^{3+}$-displaced $\{Mo^{VI}{}_2\}$/$\{Mo^{VI}{}_2(C_2H_5CO_2)\}$ linker (with a Mo···Mo distance of 3.5−3.6 Å), which would undergo a conformation change from corner- to edge-shared $MoO_6$ octahedra through the substitution of $C_2H_5CO_2^-$ by an aqua molecule. A structure similar to the $\{Mo^{VI}{}_2\}$ spacer was observed for $[\{Mo_{128}Eu_4O_{388}H_{10}(H_2O)_{81}\}_2]^{20-}$ (= $\{Mo_{128}Eu_4\}_2$) and $\{[Mo^V{}_{28}Mo^{VI}{}_{126}O_{458}H_{12}(H_2O)_{66}]^{8-}\}_\infty$ (= $\{(Mo_{154})_\infty\}$):

(21) (a) Müller, A.; Diemann, E.; Shah, S. Q. N.; Kuhlmann, C.; Letzel, M. C. *Chem. Commun.* **2002**, 440. (b) Tsuda, A.; Hirahara, E.; Kim, Y.-S.; Tanaka, H.; Kawai, T.; Aida, T. *Angew. Chem., Int. Ed.* **2004**, *43*, 6327.

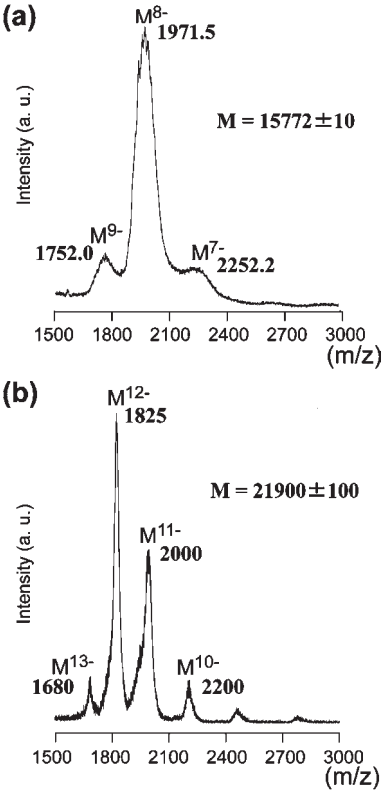


**Figure 10.** ESI-MS spectra, recorded in negative ion mode, of the aqueous solution (10 mg in 20 mL) of **2** (a) together with that (in 3 $\mu$M)) of **1**(b) in the range $m/z$ = 1500−2700. M value means the mass of the unambiguously assigned species.

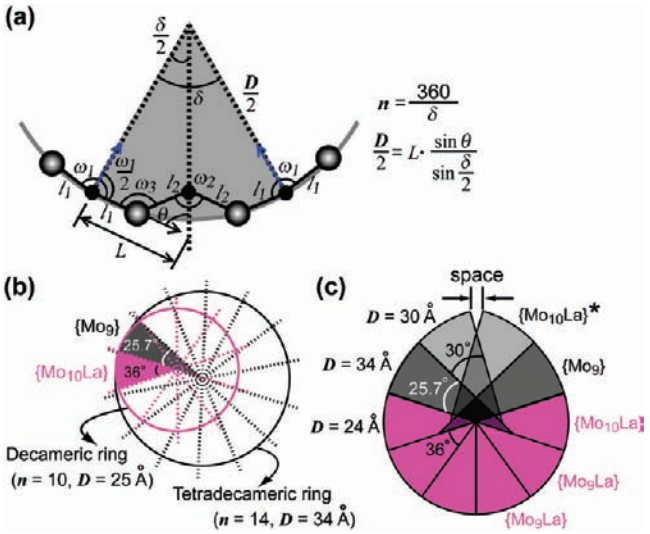


**Figure 11.** Curvature of the outer ring circle expressed by both number ($n$ in even) and ring diameter ($D$) of building subunits (a), outer ring circles (b) constructed by each building subunit of {$Mo_{10}La$} and {$Mo_9$}, and the ring profile determined by the sequence of the building subunits for **3a** (c).

the former is a dimer of two elliptical rings linked by $Eu^{3+}$ through two Mo−O−Eu−O−Mo bonds, and the elliptical ring is due to the insertion of two $[Mo^{VI}_2O_7(H_2O)]^{2-}$ spacers (at a Mo···Mo distance of 3.42 Å) into the equator.[22] In the latter of the nanotube structures, $[Mo^{VI}O_2(\mu\text{-}O)(\mu\text{-}H_2O)\text{-}Mo^{VI}O_2]^{2+}$ of the edge-shared $MoO_6$ octahedra (at a Mo···Mo distance of 3.32 Å) is inserted in each of the two inner rings as a linker.[6a] In order to understand the topology of the {$Mo_{96}La_8$} eggshell ring, the molecular curvatures of the building subunits of {$Mo_9La$}, {$Mo_{10}La$}, {$Mo_9$}, and {$Mo_{10}La$}* (as for La1 atom) were calculated by using Mo−O−Mo and O−Mo−O bond angles ($\omega_1$, $\omega_2$, and $\omega_3$) and Mo−O bond distances ($l_1$ and $l_2$) for the incomplete double-cubane-type compartment of the equator outer ring (Figures 5b and 9).[1a,7,17] Figure 11 shows the curvature of the equator outer ring (a) expressed by both the number ($n$ in even) and ring diameter ($D$) of building subunits, the outer-ring circles (b) constructed by {$Mo_{10}La$} and {$Mo_9$}, and the ring profile (c) determined by the sequence of building subunits for **3a**. Averaged values of $l_1$ and $l_2$ (in Å); $\omega_1$, $\omega_2$, and $\omega_3$ (in degrees); and the estimated values of $n$ and $D$ (in Å) for each of the building subunits in {$Mo_{96}La_8$} are listed in Table 1, where $n$ = 10, 12, and 14 indicates the formation of the closed circles corresponding to 20-$e^-$-reduced pentameric,

**Table 1.** Averaged Values of $l_1$ and $l_2$ (in Å); $\omega_1$, $\omega_2$, and $\omega_3$ (in deg); and $n$ and $D$ (in Å) for Each Equator Outer Ring of the Building Sub-Units of {$Mo_{96}La_8$}

| | {$Mo_{10}La$}* | {$Mo_9$} | {$Mo_{10}La$} | {$Mo_9La$} | {$Mo_9La$} |
|---|---|---|---|---|---|
| $l_1$ | 1.89 | 1.88 | 1.88 | 1.89 | 1.87 |
| $l_2$ | 2.03 | 2.03 | 2.05 | 2.03 | 2.03 |
| $\omega_1$ | 158 | 157 | 157 | 155 | 158 |
| $\omega_2$ | 142 | 144 | 141 | 143 | 147 |
| $\omega_3$ | 158 | 159 | 154 | 156 | 156 |
| $n$ | 12 | 14 | 10 | 10 | 10 |
| $D$ | 30 | 34 | 25 | 25 | 25 |

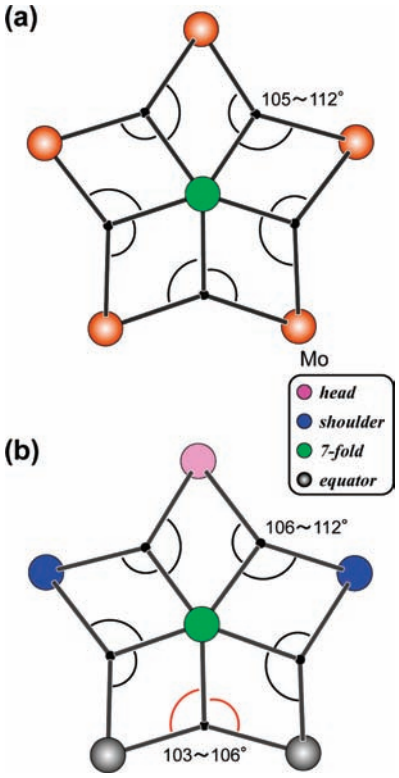


**Figure 12.** {$(Mo^{VI})(Mo^{VI}_5)O_5$} pentagons for the pentagonal subunits between **1a** (a) and {$Mo_{142}(CH_3CO_2)_5(C_2H_5CO_2)$} (b).[7] Four types (*head*, *shoulder*, *7-fold*, and *equator*) of Mo atoms are indicated by different colored balls in b.

(22) Cronin, L.; Beugholt, C.; Krickemeyer, E.; Schmidtmann, M.; Bögge, H.; Kögerler, P.; Kim, T.; Luong, K.; Müller, A. *Angew. Chem., Int. Ed. Engl.* **2002**, *42*, 2805.

24-e$^-$-reduced hexameric, and 28-e$^-$-reduced heptameric rings of $\{Mo_{20}\}/\{Mo_{21}\}/\{Mo_{22}\}$ building units, respectively. Since the electrostatic interaction of $La^{3+}$ within the negatively charged inner ring is stronger than that of the $\{Mo^{VI}_2\}$ or $\{Mo^{VI}_2(carboxylate)\}$ linker, which is less positive in charge and larger in size than $La^{3+}$, small variation of $l_1$ or $l_2$ values among the building subunits results in an increase of the molecular curvature of $\{Mo_9La\}$ and $\{Mo_{10}La\}$ with $n$ = 10 and $D$ = 25 Å due to the decrease of $\omega_1$, the increase of $\omega_2$, or the decrease of $\omega_3$, in comparison with the case of $\{Mo_9\}$ with $n$ = 14 and $D$ = 34 Å. The decreased curvature (with $n$ = 12 and $D$ = 30 Å) for $\{Mo_{10}La\}$* (Table 1) is explained by the weakened electrostatic interaction of $La^{3+}$ due to the long La1−O187′ bond distance (2.81 Å; Figures 8 and 9). One can recall that the molecular curvature of each subunit was not significantly affected by a variety of the Mo-blue rings, such as $\{Mo_{150}La_2\}$ (consisting of four $\{Mo_{10}\}$, eight $\{Mo_{11}\}$, and two $\{Mo_{11}La\}$ units), $\{Mo_{120}La_6\}$ (consisting of six $\{Mo_{10}\}$ and six $\{Mo_{10}La\}$ units), and $\{Mo_{142}(CH_3CO_2)_5(C_2H_5CO_2)\}$ (consisting of two sets of $\{Mo_9\}$, three $\{Mo_{10}\}$, four $\{Mo_{10}(carboxylate)_{1/4}\}$, three $\{Mo_{10}(carboxylate)\}$, two $\{Mo_{11}(carboxylate)_{1/2}\}$, and $\{Mo_{11}(carboxylate)\}$ subunits):[7,17] $La^{3+}$-containing subunits had $n$ = 10 and $D$ = 24−25 Å, while $\{Mo_{10}\}$, $\{Mo_{11}\}$, and their carboxylate-coordinated subunits had $n$ = 12 or 14 and $D$ = 29−30 or 34 Å. Thus, the 4-fold coordination of the inner ring to $La^{3+}$ leads to the increase in the molecular curvature of the $La^{3+}$-containing subunit with $n$ = 10 and $D$ = 24−25 Å (for $\{Mo_9La\}$, $\{Mo_{10}La\}$, and $\{Mo_{11}La\}$), and the coordination of carboxylates to the Mo-blue rings gives little effect on the molecular curvature of the subunit with $n$ = 12 or 14 and $D$ = 29−30 or 34 Å (for $\{Mo_9\}$, $\{Mo_{10}\}$, and $\{Mo_{11}\}$). The ring profile for $\{Mo_{96}La_8\}$ with two sets of the subunit sequence consisting of two $\{Mo_9La\}$, $\{Mo_{10}La\}$, $\{Mo_9\}$, and $\{Mo_{10}La\}$* subunits shows a space of approximately 1.6 Å (in agreement with the ionic diameter of $Mo^{6+}$), which excludes the possibility of closing the outer ring and rationalizes the insertion of the $\{Mo^{VI}_2\}$ spacer (Figure 11c). When $\{Mo_{10}La\}$* was replaced with $\{Mo_{10}La\}$ (with $n$ = 10 and $D$ = 24−25 Å), almost the same space remains in the ring profile, implying that the formation of the hypothetical $C_2$-$\{Mo_{94}La_8\}$ ring circle is unlikely. Similarly, it is clear that both $\{Mo_{110}\}$ (=$[Mo^{V}_{20}Mo^{VI}_{90}O_{330}(H_2O)_{50}]^{20-}$) as an intact wheel-shaped ring (consisting of 10 $\{Mo_{11}\}$ subunits with $n$ = 12 and $D$ = 29−30 Å or $n$ = 14 and $D$ = 34 Å) and its carboxylate-coordinated derivatives are unlikely. Thus, the high nuclearity Mo-blue ring of **2** (probably with a molecular weight in the range of 15194−17533) is likely to be one of the open-ring structural derivatives consisting of five 4-e$^-$-reduced building units of $\{Mo_{20}\}/\{Mo_{21}\}/\{Mo_{22}\}$ with the coordination of carboxylates, which is more flexible in the coordination to $La^{3+}$ than the closed rings with conformational rigidity.

The 60-e$^-$-reduced **1a** compound consists of 12 $\{[(Mo^{VI})Mo^{VI}_5O_{21}(H_2O)_4(C_2H_5CO_2)][Mo^{V}O_2(0.4C_2H_5CO_2 + 0.1{}^iC_3H_7CO_2)]_5\}^{4.5-}$ (=$\{[(Mo^{VI})(Mo^{VI}_5)(carboxylate)][Mo^{V}(carboxylate)_{1/2}]_5\}^{4.5-}$) pentagon units (Figure 2) and is generated formally by 60 (= 2 × 5 × 12/2) dehydration condensations (to yield the $Mo^{V}(\mu_2\text{-}O)_2Mo^{V}$ bonds accompanied by $Mo^{V}$−$Mo^{V}$ bonds) among the building blocks of the $\{[(Mo^{VI})(Mo^{VI}_5)(carboxylate)]\ [Mo^{V}O(OH)_2(carboxylate)_{1/2}]_5\}^{4.5-}$ pentagons. Since the building blocks for **1a** would be produced through the $Mo^{VI}\rightarrow Mo^{V}$ photoreduction of **2** in the presence of $C_2H_5CO_2H$, it is reasonable to assume that the $\{[(Mo^{VI})(Mo^{VI}_5)(carboxylate)]\}$ pentagonal subunit of **1a** is originated from the pentagonal subunit comprising a *head*, two *shoulder*, a *7-fold*, and two *equator* Mo atoms for **2**. The structural comparison of the pentagonal subunits between **1a** and **2** is possible by using the pentagonal subunit of $Mo\{Mo_{142}(CH_3CO_2)_5(C_2H_5CO_2)\}$ instead of **2**. Figure 12 shows the structural comparison of $\{(Mo^{VI})(Mo^{VI}_5)O_5\}$ pentagons for the pentagonal subunits between **1a** (Figure 2b) and $\{Mo_{142}(CH_3CO_2)_5(C_2H_5CO_2)\}$.[7] As shown in Figure 12, two Mo(*7-fold*)−O−Mo(*equator*) bond angles (103−106°) in $\{Mo_{142}(CH_3CO_2)_5(C_2H_5CO_2)\}$ are slightly smaller than other Mo(*7-fold*)−O−Mo(*head* and *shoulder*) angles (106−112°), which differs from **1a**, which has almost uniform Mo−O−Mo bond angles (105−112°) involving the central Mo atom. The distortion of the pentagonal subunit for $\{Mo_{142}(CH_3CO_2)_5(C_2H_5CO_2)\}$ could be attributed to the partial delocalization of the $d^1$ electron through the Mo−O−Mo linkage with a large angle (in $\omega_1$ = 158°) within the equator outer ring.[7] A similar pentagonal subunit would be predicted for **2**, in which the existence of approximately 20 $Mo^{V}$ centers (probably within the outer ring) suggests 10 pentagonal subunits (five each) above and below the equator outer ring; thus, it is inferred that the multiple $Mo^{VI}\rightarrow Mo^{V}$ photoreduction of **2** in the presence of $C_2H_5CO_2H$ occurs at the $\{Mo^{VI}_2\}/\{Mo^{VI}_2(carboxylate)\}$ linkers and/or *equator-center* Mo sites and follows the degradation of both outer-ring and binuclear linkers to yield $\{[(Mo^{VI})(Mo^{VI}_5)(carboxylate)][Mo^{V}(carboxylate)_{1/2}]_5\}^{4.5-}$ pentagon units for **1a**.

The coordination of carboxylates to both the pentagonal subunit and the peripheral linker may be significant in the formation of the Keplerates within their self-assembly, since the strong hydrophobic interaction between the carboxylates makes the molecular curvatures of $\{(Mo^{VI})(Mo^{VI}_5)(carboxylate)\}$ pentagonal subunits take an alignment among both $\{(Mo^{VI})(Mo^{VI}_5)(carboxylate)\}$ subunits and $\{Mo^{V}_2(carboxylate)\}$ linkers for the assembly toward a ball structure. The fact that most of Keplerates show the coordination of ligands such as carboxylates, sulfate, and phosphonate to either $\{(Mo^{VI})(Mo^{VI}_5)\}$ pentagonal subunits or $\{Mo^{V}_2\}$ linkers supports the importance of the hydrophobic interaction among the coordinated ligands for the assembly of a Keplerate.[15,16]

## Conclusions

The photochemical self-assembly of $[Mo_7O_{24}]^{6-}$ to $\{Mo_{132}\}$ Keplerate, $[Mo^{V}_{60}Mo^{VI}_{72}O_{372}(H_2O)_{48}(C_2H_5CO_2)_{36}({}^iC_3H_7CO_2)_6]^{54-}$ (**1a**), in the presence of a $C_2H_5CO_2H$ electron-donor at pH 4 occurs through the photoreductive degradation of the Mo-blue ring intermediate (**2**), the coordination of which to $La^{3+}$ generates the novel chain-structural eggshell rings of $\{Mo_{96}La_8\}$, $[Mo^{V}_{20}Mo^{VI}_{76}O_{301}(H_2O)_{29}\{La(H_2O)_6\}_2]\{La(H_2O)_5\}_6]^{22-}$ (**3a**). Compound **1a** is the first example in which carboxylates are coordinated to both $\{(Mo^{VI})(Mo^{VI}_5)\}$ pentagon subunits and $\{Mo^{V}_2\}$ linkers. Together with the results of the elemental analysis and IR, electronic absorption, $^{13}C$ NMR, and ESI-MS spectra for **2**, the ring profile analysis of **3a** indicates that **2** could be identified with the carbolylate-coordinated Mo-blue ring of high nuclearity (with a molecular weight in the range of 15194−17533), one of the open-ring structural derivatives probably consisting of five four-e$^-$-reduced building units of $\{Mo_{20}\}/\{Mo_{21}\}/\{Mo_{22}\}$ with the coordination of carboxylates. It is inferred

that the $Mo^{VI} \rightarrow Mo^{V}$ photoreductive change of **2** to the 60-electron-reduced Keplerate in the presence of $C_2H_5CO_2H$ involves the degradation of both outer ring and binuclear linkers, which leads to the formation of $[(Mo^{VI})Mo^{VI}_5O_{21}(H_2O)_4(carboxylate)]^{7-}$ pentagonal subunits and $[Mo^{V}_2O_4(carboxylate)]^{+}/[Mo^{V}O_2(carboxylate)_{1/2}]^{0.5+}$-mixed linkers for **1a**.

**Acknowledgment.** This work was supported by Grants-in-Aid for Scientific Research Nr. 17002006 from the Ministry of Education, Science, Sports, and Culture.

**Supporting Information Available:** Tables S1 and S2 (bond distances for **1** and **3**, respectively), Figure S1 ($^{13}C$ NMR spectra of **1** and **2** recorded at room temperature in $D_2O$) and Figure S2 (IR spectra of **2** and **3** at the range of 4000−400 $cm^{-1}$), and CIF data. These materials are available free of charge via the Internet at http://pubs.acs.org.

**Note Added after ASAP Publication.** This paper was published on the Web on September 20, 2010, with an error in ref 8. The corrected version was reposted on October 11, 2010.